NUMERICAL STUDY ON INITIAL DEFORMATION OF AN EARLY-STAGE PRESTRESSED REINFORCING BAR INSERTION METHOD

Kakuta Fujiwara[1]

[1]Department of Civil Engineering, Tokai University, Japan

ABSTRACT

Frequent earthquakes and heavy rainfall have led to numerous failures of natural and man-made slopes worldwide. Although the reinforcing bar insertion method is widely used for slope stabilization, it provides limited resistance to small initial deformations because tensile force in the reinforcing bars develops only after displacement has begun. To address this limitation, a new method, termed the “Early-stage Prestressed Reinforcing Bar Insertion Method,” is proposed. In this approach, tensile force is applied to the reinforcing bar during the grout injection and hardening stages, allowing the pressure plate to restrain the slope surface from an early stage without causing damage to the hardened grout. By introducing prestress at an early stage, the method is expected to improve the suppression of initial slope deformation. In this study, finite element numerical analyses are conducted to evaluate the effectiveness of the proposed method. The analytical results demonstrate that the proposed method can effectively reduce the initial deformation of the slope compared with the conventional method. Furthermore, it is confirmed that the deformation suppression effect is enhanced when the reinforcing bar is installed at an inclination angle of 35° from the horizontal, indicating that installation conditions play an important role in maximizing the performance of the method.

Keywords: Slope failure, Reinforcing bar insertion work, Numerical analysis, Prestress

INTRODUCTION

Across the world, numerous failures of both natural and man-made slopes have been reported due to frequent earthquakes and heavy rainfall events [1–4]. Among the various stabilization techniques applied to rock slopes, the reinforcing bar insertion method is widely recognized as one of the most commonly used approaches. In this technique, a steel bar is installed into a pre-drilled borehole, bonded to the surrounding ground using grout, and equipped with a pressure plate at the head to provide restraint. Owing to its well-established construction procedure, the method has been extensively adopted and is generally regarded as providing adequate stabilization performance [5–9]. Typically, the grout consists of ordinary cement mixed with admixtures, requiring approximately 10 hours to harden. However, immediately after installation, the reinforcing bar carries little to no axial force, and tensile resistance develops only after the slope begins to deform. Consequently, this method is less effective in restraining small initial displacements.

If tensile force could be introduced into reinforcing bars after installation, the pressure plate would press more firmly against the slope surface, potentially contributing to the suppression of initial deformations. However, there are very few studies or practical applications in which post-installation loading has been applied in reinforcing bar insertion works. According to NCHRP Report 701, reinforcing bar insertion systems are generally designed as passive systems without post-tensioning, although a limited number of special cases have applied slight tension to upper nails for deformation control [10]. One reason for this is that applying load after construction may damage the hardened grout near the bar head.

To address this issue, the present study proposes a new method termed the “Early-stage Prestressed Reinforcing Bar Insertion Work.” The objective of this method is to introduce tensile force into the reinforcing bar without causing damage to the hardened grout. This is achieved by continuously applying tensile load to the bar during the period of grout injection and hardening. By applying tension at an early stage, localized stress concentration at the head of the hardened grout can be avoided.

Fig. 1 presents the reinforcing components and construction sequence of the “Early-stage Prestressed Reinforcing Bar Insertion Method.” (a) As in the conventional reinforcing bar insertion technique, a steel bar is initially placed into a pre-drilled borehole, and its tip is fixed to the ground through primary grout injection. (b) After the grout at the tip has sufficiently hardened, a tensile force is introduced into the bar using a hydraulic jack. While maintaining this tensile state, secondary grout is injected along the remaining length to bond the bar to the surrounding ground. (c) Once this grout has hardened, the bar head is connected to a pressure plate, and the applied jack force is subsequently released, completing the installation process.

The proposed technique is original, with only one previous study on a similar concept reported by the author. In a previous study by the author [11], a construction test was conducted, confirming that the proposed method is feasible and that the tensile force in the reinforcing bar can be maintained for one month. Furthermore, numerical analyses indicated that the hardened grout body is subjected to a compressive stress state, leading to an apparent increase in its resistance to tensile loading during slope deformation. However, its effectiveness in resisting initial slope deformation has not yet been verified. Therefore, in this study, numerical analyses based on the finite element method are performed to evaluate the effectiveness of the proposed method.

RESEARCH SIGNIFICANCE

This study proposes a novel reinforcing bar insertion method in which tensile force is introduced during the grout hardening process. It has already been confirmed that this method enhances the apparent tensile strength of the hardened grout body. The present paper focuses on a supplementary effect that has not yet been clarified, namely its effectiveness in restraining initial slope deformation. The findings of this study provide a practical approach to improving stability at the early stage of slope failure and are expected to contribute to safer and more effective design and construction practices for slope stabilization.

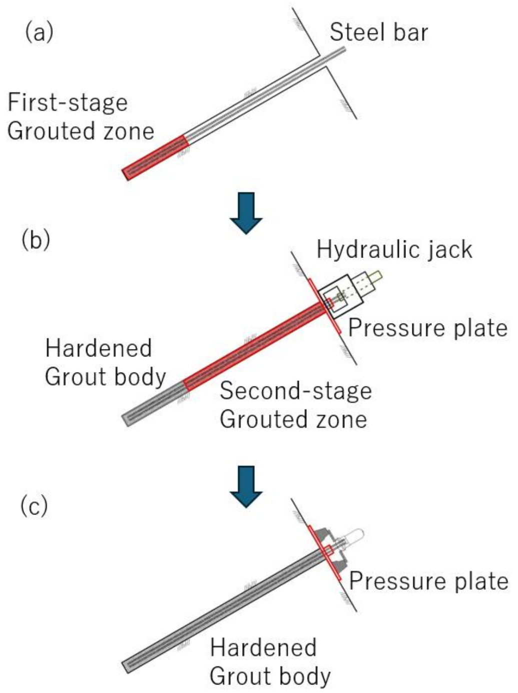

Fig.1 Early-stage prestressed reinforcing bar insertion method

NUMERICAL CONDITION

In this study, PLAXIS, a finite element program widely used for analyzing soil–structure interaction problems, is employed. It allows the simulation of slope deformation. However, due to the inherent limitations of the finite element method, large deformations associated with sliding cannot be adequately captured.

Model

The overall configuration of the analytical model is shown in Fig. 2. The coordinate system is also indicated in the same Fig. 2. The model represents a slope with a width of 18 m, a height of 11.2 m, and a depth of 2 m, with a slope angle of 35°. A horizontal section of 6 m is provided at the top of the slope, where a distributed load is applied over a width of 1.5 m at an inclination angle of 73°. The entire model is discretized using prismatic elements, resulting in 7,683 nodes and 4,298 elements. As boundary conditions, the base is fixed in all directions, while the side boundaries are constrained in the normal direction.

Case

Four analysis cases were considered in this study. Cross-sectional views of Cases 2 to 4 are shown in Fig. 3.

Case 1: No countermeasure is applied, and no reinforcement is installed. This case is used as a reference for comparison with the other cases.

Case 2: Reinforcing bars are installed perpendicular to the slope, and their heads are connected by a frame. This represents a conventional structure that is widely used in practice.

Case 3: This case corresponds to the “Early-stage Prestressed Reinforcing Bar Insertion Method”. Reinforcing bars are installed perpendicular to the slope, and pressure plates are connected at their heads. An elastic restoring force due to prestress is introduced by applying a pressure of 263 kN/m² normal to the pressure plates. This corresponds to 42 kN per reinforcing bar.

Case 4: The same method as in Case 3 is applied; however, the installation angle of the reinforcing bars is set at 35° from the horizontal.

Ground Condition

The slope consists of three layers, with a weak layer of 0.4 m thickness located between the surface layer and the bearing layer. The surface layer and weak layer are sandy soils, while the bearing layer is modeled as a rock layer. The soil properties of each layer are listed in Table 1. The Mohr–Coulomb model was applied to all three layers. Groundwater was not considered in this analysis.

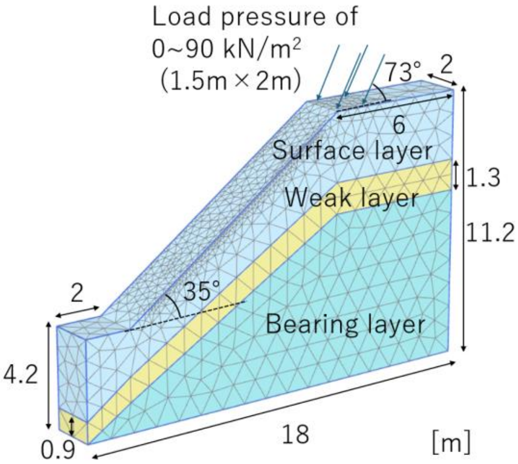

Fig.2 Numerical model

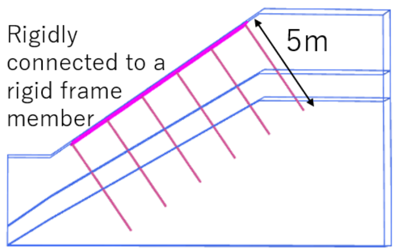

(a) Case 2

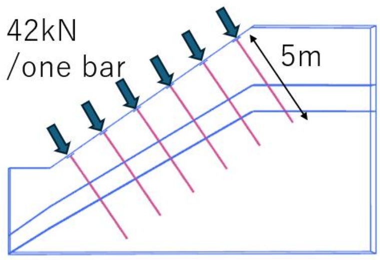

(b) Case 3

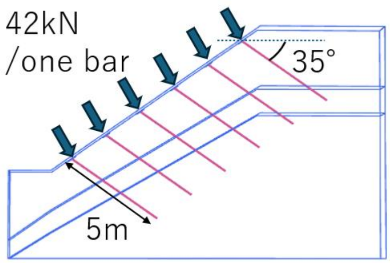

(c) Case 4

Fig.3 Numerical cases

Reinforcing bar material

The countermeasure was modeled as reinforcing bar insertion works with a length of 5 m, arranged at intervals of 2.4 m along the longitudinal direction of the slope and 2 m in the depth direction considering symmetry. The material properties of the countermeasure are listed in Table 2.

The reinforcing bar insertion work was modeled using beam elements as a composite beam consisting of a reinforcing bar and a hardened grout body. A limiting friction force of 20 kN/m was assigned between the reinforcement and the surrounding ground. The pressure plate was modeled using plate elements as a square steel plate with a side length of 40 cm. The frame members were modeled using beam elements and assumed to behave as rigid bodies. The reinforcing bars were rigidly connected to either the frame members or the pressure plate, depending on the structure.

Procedure

The analysis was carried out in the following three steps:
Step 1: A self-weight analysis of the slope with the countermeasure installed was conducted. No external load was applied.
Step 2: Surcharges of 42 kN were applied normal to the pressure plate (Cases 3 and 4).
Step 3: A load ranging from 0 to 90 kN/m² was applied incrementally to the top of the slope.

Table 1 Soil parameter

	Surface layer	Weak layer	Bearing layer
Young's modulus (kN/m^2)	3.0×10^4	1.5×10^4	5.0×10^5
Poisson's ratio	0.33	0.33	0.33
Unit weight per volume (Unsaturated) (kN/m^3)	17	17	18
Cohesion (kN/m^2)	5	5	2.0×10^4
Inner friction angle (degree)	40	40	0

Table 2 Countermeasure

	Reinforcing bar (Steel and concrete)	Pressure plate
Young's modulus (kN/m^2)	2.6×10^7	2.0×10^8
Poisson's ratio	0.33	0.33
Unit weight per volume (kN/m^3)	25	78
Diameter or Thickness (mm)	65	20
Size(mm)	L=5000	A=400×400

NUMERICAL RESULT

In this chapter, the results of each case are presented with a focus on the deformation behavior of the slope and the axial forces in the reinforcing bars.

Deformation

For each case, the contours of shear strain at the maximum applied load of 90 kN/m² are shown in Figs 4(a)–7(a), and the displacement contours are shown in Figs 4(b)–7(b).

Case 1

From the shear strain contours in Fig. 4(a), it can be confirmed that locally large strains occur beneath the applied load and within the weak layer. Focusing on the displacement contours in Fig. 4(b), downward displacement is observed mainly in the upper part of the slope, with particularly significant displacement near the slope crest. The maximum displacement reaches 18.8 mm at the crest, indicating movement in the downward direction. This displacement pattern is considered to result from the movement of the upper ground associated with shear deformation in the lower part of the slope. It should be noted that the magnitude of displacement remains sufficiently small, suggesting that the slope did not fail and that the behavior is limited to elastic–plastic deformation.

Case 2

From the shear strain contours in Fig. 5(a), it can be confirmed that the strain in the weak layer is reduced compared with Case 1. This is considered to be due to the installation of reinforcing bars, which suppress shear deformation within the weak layer. Focusing on the displacement contours in Fig. 5(b), although downward displacement of the entire slope still occurs, the maximum displacement is reduced to 14.8 mm, indicating a clear deformation suppression effect compared with Case 1. Since the reinforcing bars and frame are rigidly connected at their heads, the model represents a more constrained condition than the actual structure; nevertheless, it can be confirmed that this conventional structural system is effective in reducing slope deformation.

Case 3

From the shear strain contours in Fig. 6(a), it can be confirmed that the strain in the weak layer is slightly reduced compared with Case 1. Focusing on the displacement contours in Fig. 6(b), the maximum displacement is approximately 14.9 mm, indicating a deformation suppression effect comparable to that of Case 2. By installing reinforcing bars and applying load at their heads to restrain the ground, shear deformation in the weak layer is effectively suppressed. Fig. 8(a) shows the contours of effective stress in the ground. An increase in stress is observed in the vicinity of the countermeasure, confirming the confining effect induced by prestressing. On the other hand, the increase in stress is relatively small in the deeper part of the ground.

Case 4

From the shear strain contours in Fig. 7(a), it can be confirmed that the strain in the weak layer is clearly smaller than in the other cases. This indicates that the installation of reinforcing bars effectively suppresses shear deformation within the weak layer. Focusing on the displacement contours in Fig. 7(b), the overall downward displacement of the slope is reduced, and the maximum displacement is approximately 11.2 mm, showing the greatest deformation suppression effect among all cases. This is because the installation direction of the reinforcing bars is closer to the direction of slope deformation, allowing more direct restraint of displacement. Fig. 8(b) shows the contours of effective stress in the ground. Similar to Case 3, an increase in ground stress is observed in the vicinity of the countermeasure.

Summarize for all cases

Load-displacement relationship

The load–displacement relationships at the slope crest for all cases are shown in Fig. 9. As the load increases, the displacement also increases, exhibiting an overall approximately linear relationship, although slight nonlinearity can be observed in the high-load range. This suggests that elastic deformation is dominant under the present analytical conditions. In addition, the ranking of deformation suppression effectiveness remains unchanged at all load levels, indicating that the relative performance of each case is consistent throughout the analysis. It should be noted that this analysis is based on the finite element method, which has certain limitations in evaluating behavior in the large-strain range. Since slope failure generally involves large deformations, further studies using analytical methods capable of appropriately capturing large deformation behavior, such as the discrete element method (DEM), are required.

Axial force in reinforcement bar

The maximum tensile axial forces in the reinforcing bars for Cases 2 to 4 are shown in Fig. 10. These values correspond to the condition under a load of 90 kN/m². The horizontal axis indicates the location of the reinforcing bars, numbered from 1 to 6 from the lower part of the slope upward. For Cases 3 and 4, the values include the applied prestress of 42 kN. In all cases, tensile axial forces are generated in most of the reinforcing bars, indicating that the reinforcing bars are resisting slope deformation. In Case 2, larger tensile forces are observed at both ends, suggesting that these two bars contribute significantly to deformation suppression. In contrast, in Cases 3 and 4, the tensile forces are more evenly distributed among the reinforcing bars. Considering that the hardened grout body is relatively weak in tension, the proposed method is considered to exhibit high structural integrity.

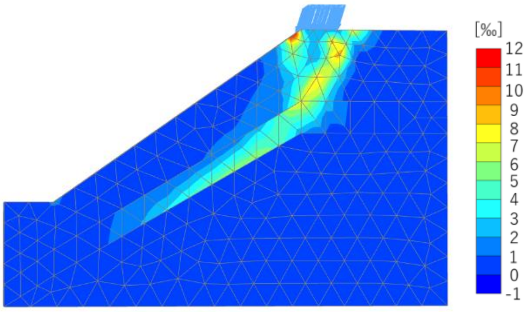

Fig.4 (a) The contour of shear strain (Case 1)

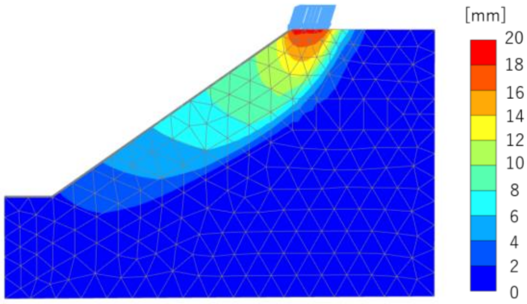

Fig.4 (b) The contour of displacement (Case 1)

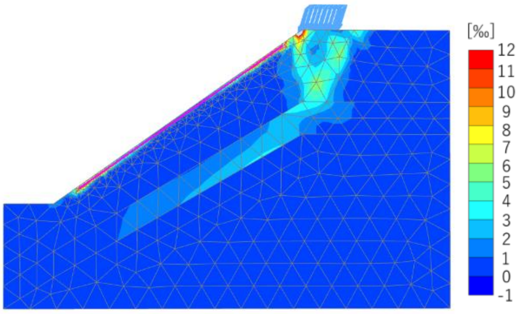

Fig.5 (a) The contour of shear strain (Case 2)

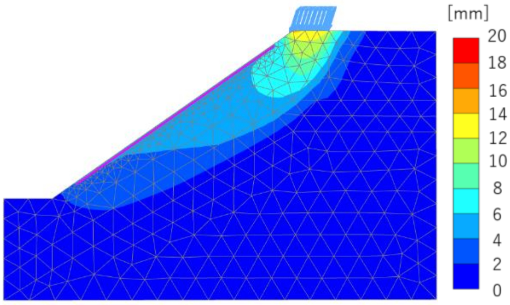

Fig.5 (b) The contour of displacement (Case 2)

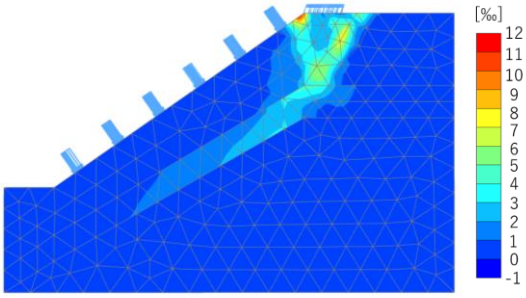

Fig.6 (a) The contour of shear strain (Case 3)

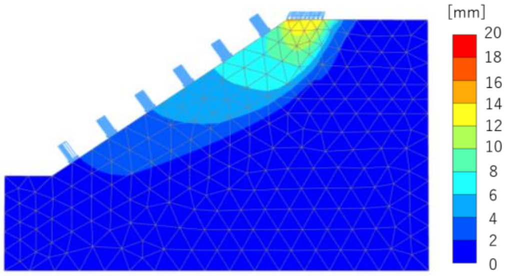

Fig.6 (b) The contour of displacement (Case 3)

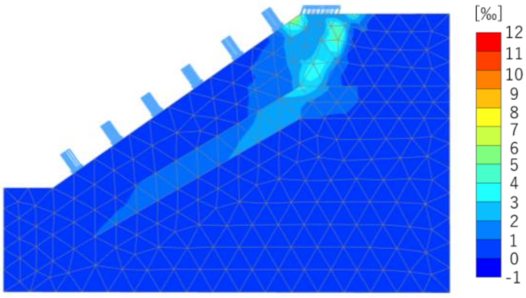

Fig.7 (a) The contour of shear strain (Case 4)

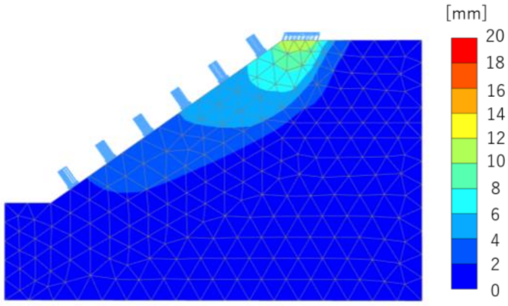

Fig.7 (b) The contour of displacement (Case 4)

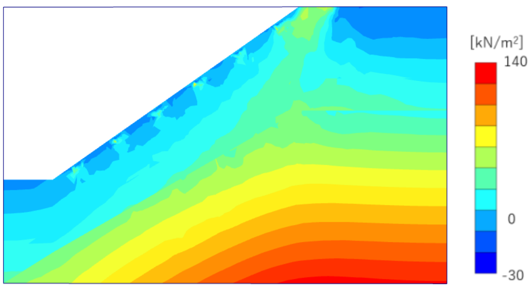

Fig.8 (a) The contour of effective stress (Case 3)

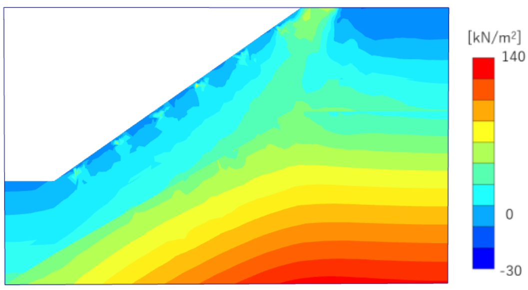

Fig.8 (b) The contour of effective stress (Case 4)

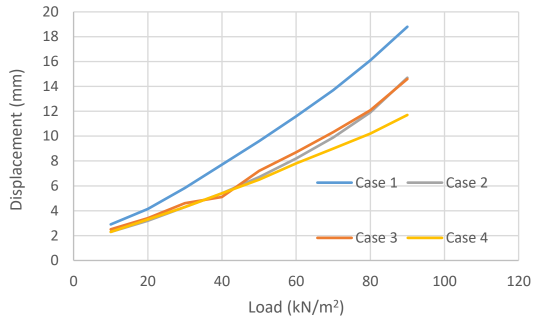

Fig.9 Load-displacement relationship

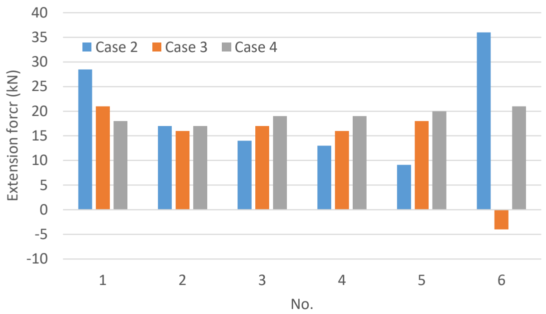

Fig.10 The tensile force in the reinforcing bar.

CONCLUSIONS

A numerical analysis based on the finite element method was conducted for the Early-stage Prestressed Reinforcing Bar Insertion Method (the proposed countermeasure). The following findings were obtained:

1) In the case without countermeasures, slope deformation induced by shear strain in the weak layer was observed under loading.

2) By connecting the heads of the reinforcing bars with a frame, as in the conventional method, the slope deformation was reduced by approximately 21%.

3) When the proposed method was applied with the reinforcing bars installed perpendicular to the slope, a reduction in slope deformation of approximately 21% was confirmed. It is expected that further deformation suppression can be achieved by increasing the prestressing load.

4) When the proposed method was applied in a direction close to the loading direction, slope deformation was reduced by approximately 40%. This is because the effective bearing area of the pressure plate against slope deformation increased, allowing more efficient resistance to deformation.

5) In the present numerical analyses, the deformation remained within small elastic and elastic–plastic ranges. Further investigation is required to evaluate behavior under large deformations, such as slope failure.

ACKNOWLEDGMENTS

This study was conducted as a collaborative research project with Chouju Reinforced Soil Co., Ltd. The author would like to express their sincere gratitude for their valuable cooperation.

REFERENCES

[1] Chiaro G., et al., Earthquake-induced flow-type slope failure: The 2016 Takanodai landslide, Japan, Geosciences, Vol. 12, 2022, pp. 394.

[2] Chowdhury F.H., et al., Modeling the Atami debris flow using a depth-integrated model, Safety in Extreme Environments, Vol. 4, 2025, pp. 45–58.

[3] Dou J., et al., Shallow and deep-seated landslide differentiation using support vector machines: Chuetsu area, Japan, Terr. Atmos. Ocean. Sci., Vol. 26, 2015, pp. 415–428.

[4] Hirata Y., et al., Landslides associated with spheroidally weathered mantle rocks during Typhoon Talas (2011) in the Kii Peninsula, Engineering Geology, Vol. 261, 2019, pp. 105–117.

[5] Fujiwara K., Wang L., Study on the effectiveness of reinforcing bar insertion work with a circular pipe, Geotechnics, Vol. 5(3), 2025, pp. 1–18.

[6] Li J., Tham L.G., Junaideen S.M., Yue Z.Q., Lee C.F., Loose fill slope stabilization with soil nails: Full-scale test, Journal of Geotechnical and Geoenvironmental Engineering, Vol. 134(3), 2008, pp. 277–288.

[7] Pradhan B., Tham L.G., Yue Z.Q., Junaideen S.M., Lee C.F., Soil-nail pull-out interaction in loose fill materials, International Journal of Geomechanics, Vol. 6(4), 2006, pp. 238–247.

[8] Junaideen S.M., Tham L.G., Law K.T., Lee C.F., Yue Z.Q., Laboratory study of soil–nail interaction in loose, completely decomposed granite, Canadian Geotechnical Journal, Vol. 41(2), 2004, pp. 274–286.

[9] Su L.-J., Chan T.C.F., Shiu Y.K., Cheung T., Yin J.H., Influence of degree of saturation on soil nail pull-out resistance in compacted completely decomposed granite fill, Canadian Geotechnical Journal, Vol. 44(11), 2007, pp. 1314–1328.

[10] National Academies of Sciences, Engineering, and Medicine, NCHRP Report 701: Proposed Specifications for LRFD Soil-Nailing Design and Construction, The National Academies Press, Washington, D.C., 2011, pp. 1–136.

[11] Fujiwara K., Construction Test and Numerical Analysis on Reinforcing Bar Insertion Method Prestressed Before Grout Hardening for Natural Slopes, Geotechnics, Vol. 5(4), 2025, 83.